Journal of Statistical Physics, Vol. 105, Nos. 5/6, December 2001 (© 2001)

New Characterization of Stochastic Resonance in Bistable Square Potential Well

Asish K. Dhara[1] **and S. R. Banerjee**[1]

Received February 2, 2001; revised July 6, 2001

The features of first passage time density function is analysed theoretically in a symmetric double square well system modulated periodically with a signal of arbitrary amplitude and frequency. Resonance is demonstrated as a maximum synchronization between periodic signal and noise. Resonance is characterized as a linear relation between noise strength at resonance and frequency. This characterization is shown to hold good for amplitude lesser or greater than the depth of the unmodulated potential well. The mean first passage time of the process at resonance is also shown to decrease linearly with the strength of the noise for high amplitude of the signal while it increases linearly with inverse of the noise strength for low amplitude.

KEY WORDS: Synchronization; stochastic resonance; first passage time density functions.

1. INTRODUCTION

There has been a great deal of interest in the understanding of mechanism of interplay between random noise and a deterministic periodic signal. It has been found that they act cooperatively in some nonlinear systems. The enhancement of the output signal power caused by injection of an optimal amount of noise into a periodically driven bistable system, commonly refered to as stochastic resonance (SR) is considered to be as one of the most puzzling and promising cooperative effects.

The phenomenon was first proposed[(1)] to explain the periodicity of the ice age by modelling the climate system as simple bistable system where each metastable state is characterized by a typical temperature. The result of the cooperative interaction of climatic fluctuation and the weak periodic

[1] Variable Energy Cyclotron Centre, 1/AF, Bidhan Nagar, Calcutta 700064, India; e-mail: akd@veccal.ernet.in

0022-4715/01/1200-0771/0 © 2001 Plenum Publishing Corporation

modulation caused by the slowly varying eccentricity of the earth is proposed to be the reason of periodic occurance of ice ages. The first realization of SR in a laboratory experiment was provided in an electronic Schmitt trigger,[2] where the circuit behaves approximately like an idealized two-state system. It was, however, only during the past decade that SR became the subject of extended investigation, mainly devoted to theoretical studies or numerical and analog simulations. SR[3] has been demonstrated in diverse systems including sensory neurons, mammalian neuronal tissue, lasers, SQUIDs, tunnel diodes and communication devices.

Characterization of SR is usually done in the following ways. Some authors[4–7, 11] described this as non-monotonous behavior of power spectrum, the signal to noise ratio, the Fourier amplitude of the periodic component of the process, while some others[12–17] observed the non-monotonous behaviour of features of the residence time distribution, as a function of the noise strength or frequency of the periodic signal.

From the theoretical point of view most of the workers assumed that either the amplitude or frequency of the periodic signal is small. This results to either linear response theory or adiabatic approximation of the process. However, some attempts have been made to remove the above restrictions on frequency either by evaluating the next order of the adiabatic approximation[8] or by considering the bistable system in the weak noise limit.[9, 10] Recently, some interesting attempt has been made to remove the restriction on frequency and noise strength by modelling the bistable system as double square well.[11] This theoretical analysis[11] demonstrates the non-monotonic dependence of the signal to noise ratio as a function of noise strength and frequency of the periodic signal with the assumption of small amplitude of the signal.

On the other hand, some workers[13, 15, 16] simulate the continuous stochastic process into a stochastic point process with the help of an analog circuit and measure the strength of the first few peaks of the residence time distribution. They observe that the residence time distribution peaks at $T_n = (n-1/2)\,T_0$ with $n = 1, 2,\ldots$ and T_0 being the period of the signal. Further, when strength of the first peak is plotted as a function of the frequency of the signal keeping noise strength constant, it hits a maximum for that period which is equal to twice of the inverse of the Kramers rate for the unbiased process at that particular noise strength. This phenomenological feature is reaffirmed recently[17] by numerical simulation of a simple two-state model, namely, periodically modulated symmetric Schmitt trigger with Gaussian noise.

In this paper we focus our attention on features of first passage time density function (FPTDF) theoretically and propose a suitable characterization of this cooperative phenomena without any restriction to amplitude

or frequency of the periodic signal. This characterization confirms our previous analytical results[18] for low amplitude of the signal.

Bistable systems used as switches are a fundamental component of electronic and optical devices. We are concerned about the response of a bistable system embedded in a noisy environment under the influence of a periodic field. The simplest model[19, 20] for the two-state spatially extended symmetric system is to consider a particle moving in the symmetric double square well potential $V(x)$ under the influence of white noise. The potential $V(x)$ is shown in Fig. 1. The influence of the external periodic field is usually described by the modulation of the potential well in the following fashion. The potential at any instant of time t for the left state is replaced by $-|V_0|+A\sin\Omega t$ and that for the right state is replaced by $-|V_0|-A\sin\Omega t$ with A, Ω being the amplitude and frequency of the periodic signal and $|V_0|$ is the barrier height when there is no modulation. To treat the problem analytically we, in particular resort to this simple model.

2. FORMULATION OF THE PROBLEM

The Fokker–Planck equation (FPE) for the probability density function $p(x, t)$ for position x of the particle at time t for this process is

$$\frac{\partial p(x,t)}{\partial t} = -\frac{\partial s(x,t)}{\partial x}, \tag{1a}$$

$$s(x,t) = -D\exp[-V(x,t)/D]\frac{\partial}{\partial x}[\exp\{V(x,t)/D\}\,p(x,t)], \tag{1b}$$

where D is strength of the white noise. It is clear that for the potential in Fig. 1, $\frac{\partial V}{\partial x}=0$ everywhere except at the discontinuous points. Therefore in each region of $V(x,t)=$constant, the FPE Eq. (1) reduces to simple diffusion equation. The solutions in each region are to be matched with the continuity of probability current and jump conditions at the discontinuous points $[-ka/2, ka/2]$ at each time. These conditions are to be supplemented by the reflecting boundary conditions at the walls $[-a(1+k/2), a(1+k/2)]$. The problem thus reduces to finding a solution of the Fokker–Planck equation with time-dependent boundary conditions. This particular feature makes the problem interesting too because no standard method to handle such problem is available in the literature.

In this paper we, however, are interested in first passage time density function (FPTDF) with mean first passage time (MFPT) being a important parameter of the process. To be specific, we concentrate on the events starting from $x=x_i=-x_f$ and ending at $x=x_f$. As the potential is symmetric,

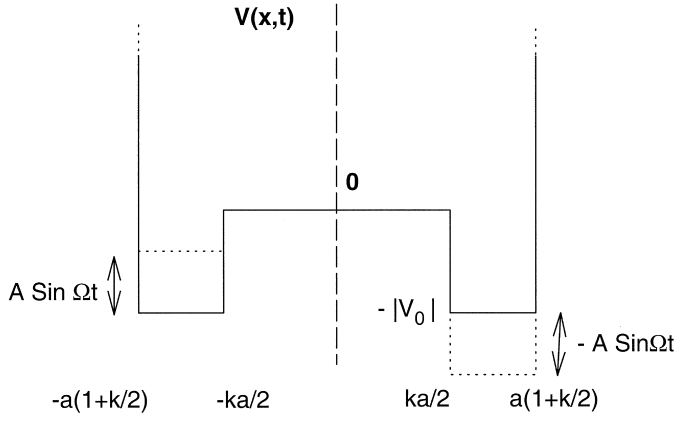

Fig. 1. Potential $V(x, t)$ at time t as a function of x.

the MFPT $\langle t(-x_f \to x_f)\rangle$ would be same as $\langle t(x_f \to -x_f)\rangle$. The conditions that the required solution of Eq. (1) satisfies are:

$$p'(-a(1+k/2), t) = 0, \tag{2a}$$

$$e^{[-|V_0|+A\sin \Omega t]/D} p(-ka/2-0, t) = p(-ka/2+0, t), \tag{2b}$$

$$p'(-ka/2-0, t) = p'(-ka/2+0, t), \tag{2c}$$

$$p(ka/2-0, t) = e^{[-|V_0|-A\sin \Omega t]/D} p(ka/2+0, t), \tag{2d}$$

$$p'(ka/2-0, t) = p'(ka/2+0, t), \tag{2e}$$

$$p(x_f, t) = 0, \tag{2f}$$

where prime over p in the above equations denote derivative with respect to x. Equation (2a) corresponds to reflecting boundary condition for the wall at $x = -a(1+k/2)$. As $\lim_{\delta \to 0} \int_{\pm ka/2-\delta}^{\pm ka/2+\delta} e^{V/D} s(x, t)\, dx$ vanishes, we obtain the jump conditions Eqs. (2b) and (2d) at the discontinuous points $x = \pm ka/2$. Noting that $\lim_{\delta \to 0} \int_{\pm ka/2-\delta}^{\pm ka/2+\delta} \frac{\partial s}{\partial x}\, dx = -\lim_{\delta \to 0} \frac{\partial}{\partial t} \int_{\pm ka/2-\delta}^{\pm ka/2+\delta} p(x, t)\, dx$, and assuming that the probability to find a particle in the interval 2δ goes to zero for $\delta \to 0$, the matching condition Eqs. (2c) and (2e) for continuity of probability current at the discontinuous points $x = \pm ka/2$ are obtained. Equation (2f) is the absorbing boundary condition at $x = x_f$ for the process considered.

No analytic solution exists for Eq. (1) with the boundary conditions given by Eq. (2). We thus introduce a scheme to approximate the force $\sin \Omega t$ as a multi-step periodic signal.[21]

The construction of multi-step periodic signal is as follows. We divide the half cycle of the signal by $(2p+1)$ intervals so that each interval in the horizontal t-axis is of size $(\triangle t/(2p+1))$ with $\Omega \triangle t = \pi$. We define $(2p+1)$ numbers s_k along the vertical axis as

$$s_k = \frac{\left[\sin\frac{k\pi}{2p+1} + \sin\frac{(k-1)\,\pi}{2p+1}\right]}{2}; \qquad k = 1, 2,\ldots, p \tag{3a}$$

$$s_{p+1} = 1 \tag{3b}$$

$$s_{p+1+r} = s_{p+1-r}; \qquad r = 1, 2,\ldots, p. \tag{3c}$$

Each number s_k is associated with the interval $\frac{(k-1)\triangle t}{2p+1} < t \leqslant \frac{k\triangle t}{2p+1}$ with $k = 1, 2,\ldots, (2p+1)$. Equation (3) clearly shows that

$$0 < s_1 < s_2 < \cdots < s_p < s_{p+1} = 1 > s_{p+2} > s_{p+3} > \cdots > s_{2p+1} > 0. \tag{4}$$

Equation (4) states that in order to reach the maximum value ($= 1$) of the signal from the zero level we have to have $(p+1)$ step up and from the maximum to the zero level we have $(p+1)$ step down. This is for the positive half-cycle. For the negative half-cycle similar constructions have been done with the replacement $s_k \to -s_k$, $\forall k$ and each number $-s_k$ is associated with the interval $\triangle t[1+\frac{k-1}{2p+1}] < t \leqslant \triangle t[1+\frac{k}{2p+1}]$ with $k = 1, 2,\ldots,$ $(2p+1)$. This aproximation for the full one cycle of the sinusoidal signal (as shown in Fig. 2) is then repeated for the next successive cycles.

One may, however, note that the Ω which we have defined for this approximated signal is not the same as that of sinusoidal signal, because the Fourier transform of sinusoidal signal would give only one frequency while this approximated signal in the Fourier space corresponds to many sinusoidal frequencies, especially because of its sharp discontinuities. Yet we urge this approximation because in each small interval the boundary conditions become time-independent. Further, we can choose the infinitesimal time interval as small as we please by increasing the number of steps of multi-step periodic signal.

In the future development the index i will refer to the cycle number. With the help of multi-step periodic signal in each small time interval the conditional probability density function $p(x, t \mid x', t')$ could be expressed as

$$p(x, t \mid x', t') = \sum_n \psi_n(x)\, \psi_n(x') \exp[-\lambda_n(t-t')], \tag{5}$$

where $\psi_n(x)$ are the normalised eigenfunctions functions and the corresponding eigenvalues are denoted as λ_n. Substituting Eq. (5) into Eq. (1) one obtains

$$\frac{\partial^2\psi_n(x)}{\partial x^2} = -(\lambda_n/D)\, \psi_n(x). \tag{6}$$

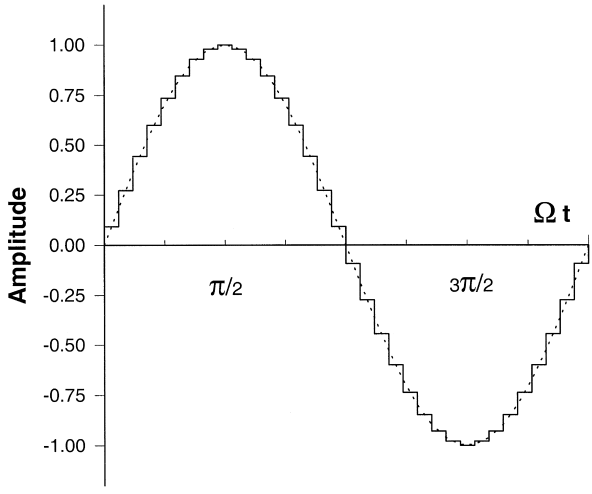

Fig. 2. Sinusoidal signal (dashed curve) and approximated multi-step ($p = 8$) periodic signal (solid curve) for the full one cycle as a function of time.

Substituting Eq. (5) into the matching conditions Eqs.(2a)–(2f) one obtains the following set of conditions for $\psi(x)$ with the help of multi-step periodic signal defined in Eq. (3):

$$\psi_n'(-a(1+k/2)) = 0, \tag{7a}$$

$$e^{[-|V_0|+\epsilon]/D}\psi_n(-ka/2-0) = \psi_n(-ka/2+0), \tag{7b}$$

$$\psi_n'(-ka/2-0) = \psi_n'(-ka/2+0), \tag{7c}$$

$$\psi_n(ka/2-0) = e^{[-|V_0|-\epsilon]/D}\psi_n(ka/2+0), \tag{7d}$$

$$\psi_n'(ka/2-0) = \psi_n'(ka/2+0), \tag{7e}$$

$$\psi_n(x_f = a(1+k)/2) = 0, \tag{7f}$$

where $\epsilon = A.s$ with s being the corresponding value of s_k defined by Eq. (3) in the appropriate time interval where the conditional probability density is being decomposed. The solutions of Eq. (6) in each region of the potential are obtained. They express as

$$\psi_n(x) = C_n \cos\{k_n[x+a(1+k/2)]\}; \quad -a(1+k/2) \leqslant x < -ka/2, \tag{8a}$$

$$\psi_n(x) = C_n^{(2)} \sin(k_n x) + C_n'^{(2)} \cos(k_n x); \quad -ka/2 < x < ka/2, \tag{8b}$$

$$\psi_n(x) = C_n^{(3)} \sin(k_n x) + C_n'^{(3)} \cos(k_n x); \quad ka/2 < x \leqslant x_f, \tag{8c}$$

where $C_n^{(2)}$, $C_n'^{(2)}$, $C_n^{(3)}$ and $C_n'^{(3)}$ are given by

$$\begin{aligned} C_n^{(2)} &= -C_n[(\beta/\alpha)\cos(k_n a)\sin(k_n ka/2) \\ &\quad +\sin(k_n a)\cos(k_n ka/2)], \end{aligned} \tag{9a}$$

$$\begin{aligned} C_n'^{(2)} &= C_n[(\beta/\alpha)\cos(k_n a)\cos(k_n ka/2) \\ &\quad -\sin(k_n a)\sin(k_n ka/2)], \end{aligned} \tag{9b}$$

$$\begin{aligned} C_n^{(3)} &= C_n[\beta^2\cos(k_n a)\sin(k_n ka/2)\cos(k_n ka) \\ &\quad -\sin(k_n a)\cos(k_n ka/2)\cos(k_n ka) \\ &\quad -2\alpha\beta\sin(k_n a)\sin^2(k_n ka/2)\cos(k_n ka/2) \\ &\quad -2(\beta/\alpha)\cos(k_n a)\cos^2(k_n ka/2)\sin(k_n ka/2)], \end{aligned} \tag{9c}$$

$$\begin{aligned} C_n'^{(3)} &= C_n[\beta^2\cos(k_n a)\cos(k_n ka/2)\cos(k_n ka) \\ &\quad +\sin(k_n a)\sin(k_n ka/2)\cos(k_n ka) \\ &\quad -2\alpha\beta\sin(k_n a)\cos^2(k_n ka/2)\sin(k_n ka/2) \\ &\quad +2(\beta/\alpha)\cos(k_n a)\sin^2(k_n ka/2)\cos(k_n ka/2)], \end{aligned} \tag{9d}$$

where $k_n^2 = \lambda_n/D$, $\alpha = e^{|V_0|/D}$, $\beta = e^{\epsilon/D}$, and the constant C_n is determined from the normalisation condition

$$C_n^2 \int_{-a(1+k/2)}^{x_f} \psi_n^2(x)\,dx = 1. \tag{10}$$

The corresponding eigenvalues are determined from the transcendental equation

$$L(\alpha) + L(\beta) = 0, \tag{11}$$

where $L(\alpha)$ and $L(\beta)$ are given by

$$\begin{aligned} L(\alpha) &= \cos(k_n ka)\cos\{k_n[x_f + a(1-k/2)]\} \\ &\quad -\alpha\sin(k_n ka)\sin(k_n a)\cos\{k_n(x_f - ka/2)\} \\ &\quad -(1/\alpha)\sin(k_n ka)\cos(k_n a)\sin\{k_n(x_f - ka/2)\}, \end{aligned} \tag{12a}$$

$$\begin{aligned} L(\beta) &= (\beta-1)\cos(k_n ka)\cos(k_n a)\cos\{k_n(x_f - ka/2)\} \\ &\quad +(1-\beta^{-1})\cos(k_n ka)\sin(k_n a)\sin\{k_n(x_f - ka/2)\}. \end{aligned} \tag{12b}$$

The conditional probability density function in any time interval, say l, can then be calculated from the previous history by convoluting it in each previous intervals:

$$p(x_l, t_l \mid x_1, t_1) = \int \cdots \int dx_{l-1}\, dx_{l-2} \cdots dx_2 \prod_{j=2}^{l} p(x_j, t_j \mid x_{j-1}, t_{j-1}). \tag{13}$$

The survival probability at time t , $S(t \mid t_0; -x_f)$ can be obtained as

$$S(t \mid t_0; -x_f) = \int_{-a(1+k/2)}^{x_f} p(x, t \mid -x_f, t_0)\, dx, \tag{14}$$

and the first passage time density function (FPTDF) $g(t \mid t_0)$ is obtained from $S(t \mid t_0; -x_f)$ as

$$g(t \mid t_0) = -\frac{dS(t \mid t_0; -x_f)}{dt}. \tag{15}$$

Physically, $g(t \mid t_0)\, dt$ gives the probability that the particle reaches $x = x_f$ for the first time in the time interval t and $t + dt$ starting from $x = -x_f$ at $t = t_0$. Different moments of $g(t \mid t_0)$ can be readily calculated from the normalised $g(t \mid t_0)$ as

$$\langle (t - t_0)^j \rangle = \int_{t_0}^{\infty} (t - t_0)^j\, g(t \mid t_0)\, dt; \qquad j = 1, 2, \ldots. \tag{16}$$

It is to be noted that as the matching conditions are changing with time through the value of s, the probability density function would not be homogeneous in time. It would depend explicitly on initial time t_0. In experiment, however, it is difficult to control the initial time t_0. One therefore should take the average of the probability distribution function with respect to initial time t_0. If t_0 is chosen with uniform probability over the signal period T_0, we would get the average conditional probability distribution function as

$$\langle p(x, \tau \mid -x_f) \rangle = \frac{1}{T_0} \int_0^{T_0} dt_0\, p(x, t_0 + \tau \mid -x_f, t_0). \tag{17}$$

With this average value of the conditional probability various moments can similarly be calculated.

It is then quite straight-forward to calculate the survival probability at any time interval of any cycle. We will write down the final formulae:

$$S_{i,k}(t \mid x_i; t_0) = C_{n_{i,k}} \times O_k(\psi_{n_{i,k}}) \times \exp[-\lambda_{n_{i,k}}(t - 2(i-1)\triangle t)],$$
$$; \left[2(i-1) + \frac{k-1}{2p+1}\right]\triangle t < t \leqslant \left[2(i-1) + \frac{k}{2p+1}\right]\triangle t,$$
$$; k = 1, 2, \ldots, 2(2p+1), \tag{18}$$

where

$$C_{n_{i,k}} = \int_{-a(1+k/2)}^{x_f} dx\, \psi_{n_{i,k}}(x), \tag{19}$$

and the functions O_k are generated through the recursion relations:

$$O_1(\psi_{n_{(i+1),1}}) = F_{i+1}(\psi_{n_{(i+1),1}}), \tag{20a}$$

$$O_k(\psi_{n_{i,k}}) = \langle \psi_{n_{i,k}} \mid \psi_{n_{i,(k-1)}} \rangle \times \exp\left[\frac{(k-1)\triangle t}{2p+1}(\lambda_{n_{i,k}} - \lambda_{n_{i,(k-1)}})\right]$$
$$\times O_{k-1}(\psi_{n_{i,(k-1)}}),$$
$$; k = 2, 3, \ldots, 2(2p+1), \tag{20b}$$

$$F_{i+1}(\psi_{n_{(i+1),1}}) = \langle \psi_{n_{(i+1),1}} \mid \psi_{n_{i,2(2p+1)}} \rangle \times \exp[-2\lambda_{n_{i,2(2p+1)}}\triangle t]$$
$$\times O_{2(2p+1)}(\psi_{n_{i,2(2p+1)}}), \tag{20c}$$

with the definition $n_{i,k} \equiv n_{2(2p+1)(i-1)+k}$ and $O_l(\psi_{n_{1,l}}) = \psi_{n_{1,l}}(x_i).e^{\lambda_{n_{1,l}}t_0}$ for $(l-1)\triangle t/(2p+1) \leqslant t_0 \leqslant l\triangle t/(2p+1)$; $l = 1, 2, \ldots, 2(2p+1)$. The angular bracket in any equation implies dot product of the corresponding functions, for, e.g.,

$$\langle \psi_{n_{i,k}} \mid \psi_{n_{j,l}} \rangle = \int_{-a(1+k/2)}^{x_f} dx\, \psi_{n_{i,k}}(x).\psi_{n_{j,l}}(x). \tag{21}$$

The cycle variable i runs over positive integers; i.e., $i = 1, 2, 3, \ldots$. In all these expressions, viz., Eqs. (18)–(20), any running subscript appeared more than once, the summation over that is implied. The summation corresponds to the summation over the eigenvalues as in spectral decomposition of conditional probability. The effect of history is explicit in the expressions for survival probabilities. Once the survival probability $S(t \mid x_i; t_0)$ is obtained from these formluae, the FPTDF, MFPT and the corresponding variance are obtained by employing Eqs. (15) and (16). Evaluation of

MFPT and other relevant quantities requires sum of infinite series which must be truncated in order to obtain a final result. Convergence of MFPT is ensured by gradually increasing the number of terms (i.e., number of eigenvalues) for the calculation. The process is truncated when MFPT does not change upto two decimal point of accuracy with the change of number of terms.

3. RESULTS AND DISCUSSIONS

The calculations are done with the potential parameters $a = 4$, $k = 2$, $|V_0| = 0.25$, $A = 0.2$ and 0.4. We have chosen these two representative amplitudes ($A = 0.2$ and 0.4) since in this general formalism (arbitrary amplitude) they represent one case with low amplitude ($A = 0.2$) and the other with high amplitude ($A = 0.4$) compared to the depth $|V_0|$ of the potential well. The sinusoidal signal is approximated with $p = 8$ (17 steps in one half cycle) [Eq. (3)] multistep periodic signal in our calculation. The particle is assumed to start at $t_0 = 0$ from the initial point $x_i = -6$ (mid point of the left well) and ends its journey at $x_f = 6$ (mid point of the right well). Normalized FPTDF $g(t) \equiv g(t \mid 0)$ as a function of t/T_0 for a fixed value of the signal frequency $\Omega = 0.2$, amplitude $A = 0.4$ and different values of $D/|V_0|$ are plotted in Fig. 3. The results of the calculation with $A = 0.2$ are not shown here as the features are similar to those for the high amplitude ($A = 0.4$) case. The results with the low amplitude case also confirms our previous results[18] obtained through an asymptotic expansion of probability distribution function. In Fig. 3 multiple peaks are observed for small values of the noise strength and as noise strength increases, the background over which the peaks occur also increases.The peak heights fall exponentially with time for fixed $D/|V_0|$ and for small noise strengths they take larger values. Successive peaks are separated by a time interval exactly equal to the period of the signal T_0 showing that the probability of transition is maximum after each period. At these particular times the synchronization between the deterministic periodic force and the random noise is maximum helping the particle to reach the terminating point at the right well by overcoming the barrier. Peak areas are also found to be decreasing with time. The peak areas are a good measure of the synchronization[18] and directly gives the probability of transition within the time interval.

We calculate the peak areas by integrating around the nth peak after subtracting the background ($P_n = \int g(t)\, dt$). The peak areas are plotted as a function of $D/|V_0|$ in Fig. 4. The figure demonstrates a non-monotonous behaviour for each peak exhibiting a signature of maximum cooperation or synchronization between the noise and the external frequency at specific

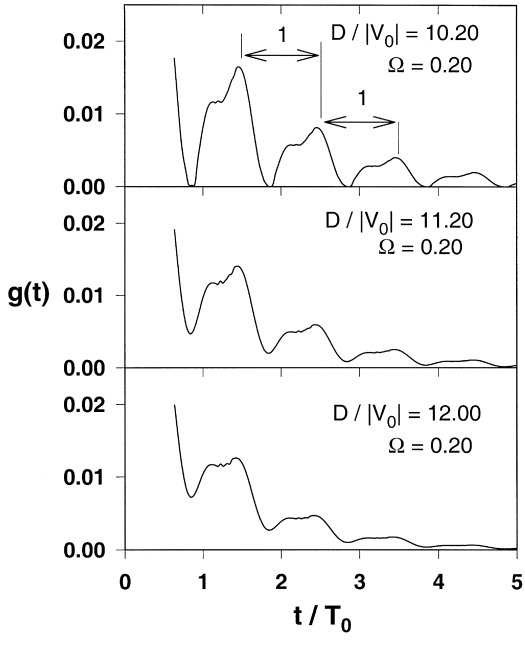

Fig. 3. FPTDF $g(t)$ as a function of t/T_0 for frequency $\Omega = 0.2$ and $D/|V_0| = 10.20$, 11.20, 12.0 for amplitude $A = 0.4$.

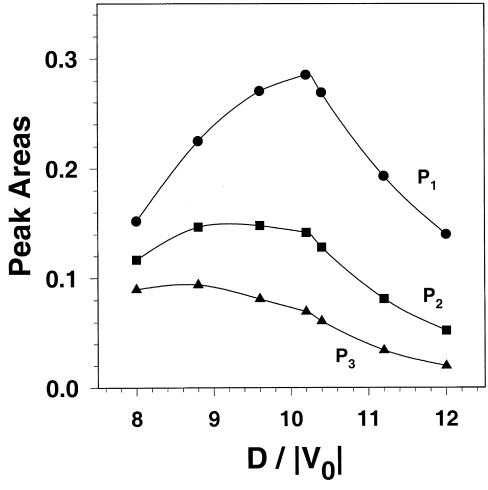

Fig. 4. Peak areas as a function of $D/|V_0|$ for $\Omega = 0.2$ and $A = 0.4$.

values of noise strength for a particular signal frequency. Also the degree of synchronization is gradually lesser for second, third etc. peaks respectively.

In a similar manner, for a fixed $D/|V_0| = 10.20$, amplitude $A = 0.4$, the normalized FPTDF $g(t)$ are plotted for different signal frequencies in Fig. 5. It also shows similar behavior like already discussed (Fig. 3). The area of the first and the most dominant peak (integrated after background subtraction) is plotted as a function of the signal frequency in Fig. 6. It also exhibits a similar non-monotonous behaviour and shows that synchronization is maximum at a particular signal frequency for a given $D/|V_0|$. This is so called resonant behaviour and the specific values of the noise strengths and the signal frequencies are denoted by D_{res} and Ω_{res} respectively.

Three dimensional plots of dominant peak areas P_1 as a function of noise strength D and frequency Ω for different amplitudes $A = 0.4$ (larger than the depth of the unperturbed potential) and $A = 0.2$ (smaller than the depth of the unperturbed potential) are given in Fig. 7. These would demonstrate the global view. This figure represents the fitted surface from the calculated peak areas for different frequencies and noise strengths. The maximum peak areas correspond to maximum synchronization between

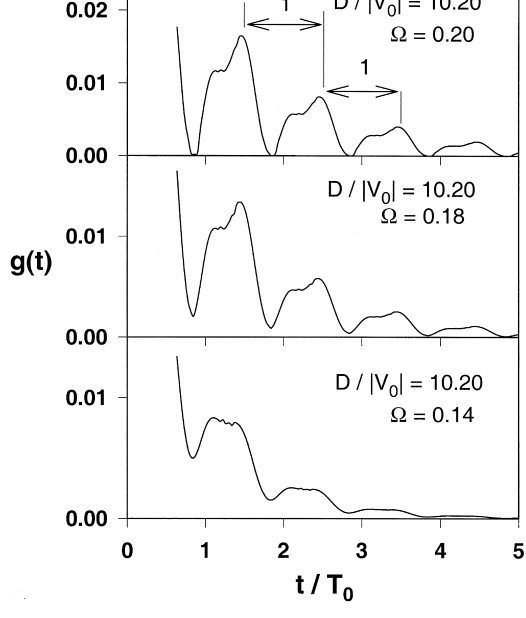

Fig. 5. FPTDF $g(t)$ as function of time t/T_0 for $D/|V_0| = 10.20$ and $\Omega = 0.14, 0.18, 0.20$.

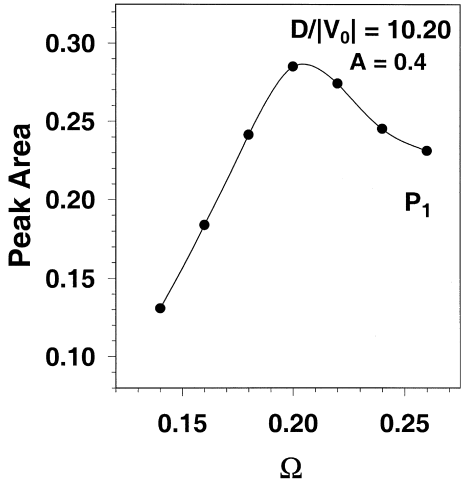

Fig. 6. Peak area as a function of Ω for $D/|V_0| = 10.20$ and $A = 0.4$.

noise and periodic signal and referred to as resonance condition. The typical sections for given frequency and for given noise strength of this three dimensional plot are shown in Figs. 4 and 6 respectively. In order to demonstrate the nonmonotonous behavior of peak areas P_1 versus noise strength D for given frequency and that against frequency Ω for given noise strength we make suitable cuts along frequency and noise strength axes of Fig. 7a and draw the three dimensional plot Fig. 7b for amplitude $A = 0.4$. Similar figure could be obtained for amplitude $A = 0.2$.

As MFPT is a very important time scale in the noise induced transition, we evaluate MFPT averaged over initial time at resonance using Eqs. (16) and (17) and plot as a function of noise strength for both high ($A = 0.4$) and low ($A = 0.2$) amplitudes in Fig. 8. These curves are compared with the MFPT vs. noise strength curve when there is no signal in the same figure. The curves show that the MFPT is more for resonance case than that for no-bias case. As amplitude A corresponds to the strength of the signal, for given noise strength D, it is expected that the frequency of occurance of the maximum strength (size of the signal) would be more for low amplitude than that for high amplitude to combat the strength of the noise for resonance to occur. As amplitude increases, the MFPT to reach the right well is found to decrease as expected. The interesting point to note that at resonance for high amplitude ($A = 0.4$) the MFPT decreases linearly with the noise strength while for low amplitude ($A = 0.2$) the MFPT increases linearly with the inverse of the noise strength.

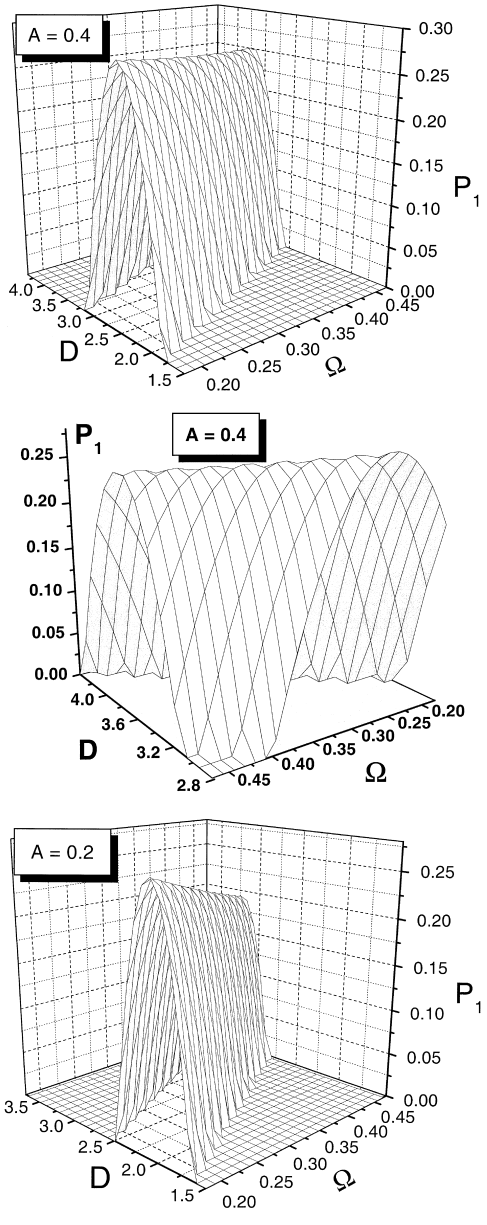

Fig. 7. (a) Peak areas P_1 as a function of frequency Ω and noise strength D for signal amplitude $A = 0.4$. (b) Peak areas P_1 as a function of frequency Ω and noise strength D with suitable cuts along D and Ω axes (see the text) for signal amplitude $A = 0.4$. (c) Peak areas P_1 as a function of frequency Ω and noise strength D for signal amplitude $A = 0.2$.

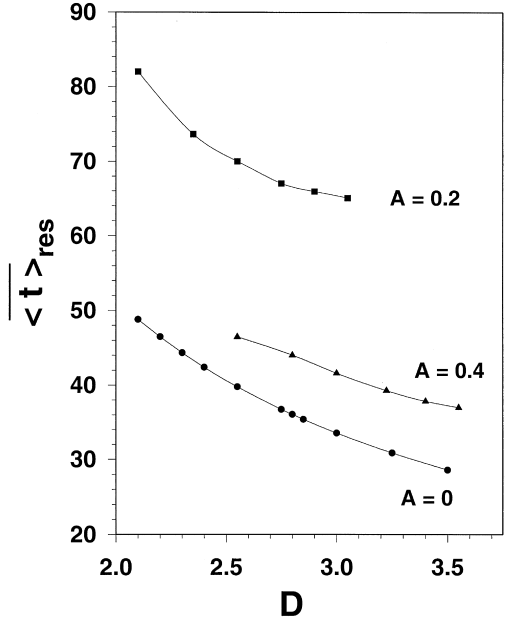

Fig. 8. MFPT at resonance $\overline{\langle t \rangle_{\text{res}}}$ as a function of strength of the noise D with signal ($A = 0.4$) [line with filled triangles], ($A = 0.2$) [line with filled squares], and without signal ($A = 0$) [line with filled circles].

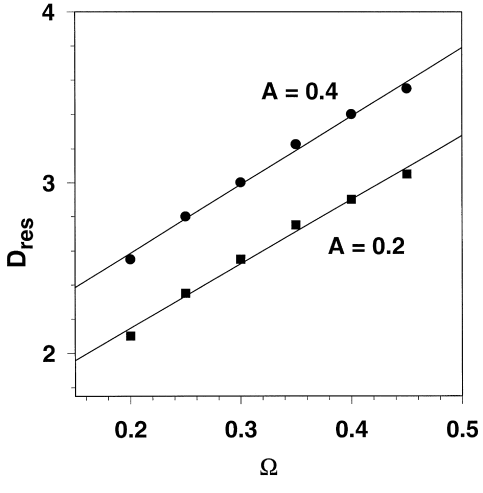

Fig. 9. Noise strength at resonance D_{res} as a function of frequency Ω for $A = 0.2$ [line with filled squares] and $A = 0.4$ [line with filled circles].

We have seen that the synchronization is maximum for specific noise strengths for different signal frequencies and vice versa. The values of the noise strengths at resonance (D_{res}) are plotted as a function of the signal frequency Ω in Fig. 9 for two different cases, e.g., $A = 0.2$ and $A = 0.4$. They show linear behaviour but with different slopes—the one with higher amplitude is steeper. We fit two straight lines through these points and they give, $D_{res} = 3.77\Omega + 1.39$ (for $A = 0.2$) and $D_{res} = 4.01\Omega + 1.78$ (for $A = 0.4$). This shows that as the frequency of the signal increases, the noise strength for which the resonance occurs also increases linearly. This could be understood as follows. Suppose the system is at resonance; the state of the system is defined by a particular frequency and noise strength (D_{res}). If the noise strength is increased maintaining the frequency constant, Fig. 3 suggests that the system becomes in off-resonant condition. The background area increases and correspondingly the peak area over the background decreases. In order to drive the system in resonant condition again with this increased value of noise strength, the background area should be decreased. This is achieved by increasing the frequency as suggested from Fig. 5. At resonance, the optimal noise strength is related to the driving frequency. In symmetric bistable square well, we find that the dependence is linear. The linear relation between the optimal noise intensity and the driving frequency is important because this fact might help the experimentalists in studying the resonance behaviour in complex systems where tuning the frequency is a convenient task than varying the internal noise or temperature.

In conclusion, in this paper we propose a new characterization of the stochastic resonance in bistable square potential well. Resonance is characterized as a linear relation between noise strength at resonance and the frequency of the periodic signal. This characterization is shown to hold good for amplitudes lesser or greater than the depth of the unmodulated potential well. Although we found this characterization for bistable square potential well for the sake of analytic treatment of the process for arbitrary amplitudes, we believe this simple linear relationship would hold good for general bistable potential as well.

REFERENCES

1. R. Benzi, A. Sutera, and A. Vulpiani, *J. Phys. A* **14**:453 (1981); R. Benzi, G. Parisi, A. Sutera, and A. Vulpiani, *Tellus* **34**:10 (1982); C. Nicolis and G. Nicolis, *Tellus* **33**:225 (1981).
2. S. Fauve and F. Heslot, *Phys. Lett. A* **97**:5 (1983).
3. B. McNamara, K. Wiesenfeld, and R. Roy, *Phys. Rev. Lett.* **60**:2626 (1988); G. Vemuri and R. Roy, *Phys. Rev. A* **39**:4668 (1989); F. Moss, A. Bulsara, and M. Schlesinger, Proceedings of the NATO Advanced Research Workshop on Stochastic Resonance in Physics

and Biology, *J. Statist. Phys.* **70** (1/2) (1993); K. Wiesenfeld and F. Moss, *Nature (London)* **373**:33 (1995); A. Bulsara and L. Gammaitoni, *Phys. Today* **49**:39 (1996); L. Gammaitoni, P. Hänggi, P. Jung, and F. Marchesoni, *Rev. Mod. Phys.* **70**:223 (1998). M. Grifoni and P. Hänggi, *Phys. Rep.* **304**:229 (1998).

4. B. McNamara and K. Wiesenfeld, *Phys. Rev. A* **39**:4854 (1989).
5. Hu Gang, G. Nicolis, and C. Nicolis, *Phys. Rev. A* **42**:2030 (1990).
6. P. Jung and P. Hänggi, *Europhys. Lett.* **8**:505 (1989).
7. P. Jung and P. Hänggi, *Phys. Rev. A* **44**: 8032 (1991).
8. G. Hu, H. Haken, and C. Z. Ning, *Phys. Lett. A* **172**:21 (1992).
9. V. A. Shneidman, P. Jung, and P. Hänggi, *Phys. Rev. Lett.* **72**:2682 (1994).
10. N. G. Stocks, *Nuovo Cimento D* **17**:925 (1995).
11. V. Berdichevsky and M. Gitterman, *J. Phys. A: Math. Gen.* **29**:L447 (1996).
12. T. Zhou, F. Moss, and P. Jung, *Phys. Rev. A* **42**:3161 (1990).
13. L. Gammaitoni, F. Marchesoni, and S. Santucci, *Phys. Rev. Lett.* **74**:1052 (1995).
14. G. Giacomelli, F. Marin, and I. Rabbiosi, *Phys. Rev. Lett.* **82**:675 (1999).
15. L. Gammaitoni, F. Marchesoni, E. Menichella-Saetta, and S. Santucci, *Phys. Rev. E* **51**: R3799 (1995).
16. F. Apostolico, L. Gammaitoni, F. Marchesoni, and S. Santucci, *Phys. Rev. E* **55**:36 (1997).
17. F. Marchesoni, L. Gammaitoni, F. Apostolico, and S. Santucci, *Phys. Rev. E* **62**:146 (2000).
18. Asish K. Dhara and S. R. Banerjee, *J. Statist. Phys.* **99**:799 (2000).
19. M. Mörsch, H. Risken, and H. D. Vollmer, *Z. Physik B* **32**:245 (1979).
20. V. Berdichevsky and M. Gitterman, *Phys. Rev. E* **59**:R9 (1999).
21. Asish K. Dhara and Tapan Mukhopadhyay, *Phys. Rev. E* **60**:2727 (1999).